


## Tuning electronic and magnetic properties of the graphone/Ni(111) interface by oxygen intercalation: A first-principles prediction

Niharika Joshi <sup>1,\*</sup>, C. Gaurav,<sup>2</sup> Nirmalya Ballav,<sup>1</sup> and Prasenjit Ghosh<sup>3</sup>

<sup>1</sup>Department of Chemistry, Indian Institute of Science Education and Research, Pune-411008, India

<sup>2</sup>Department of Physics, Indian Institute of Science Education and Research, Pune-411008, India

<sup>3</sup>Department of Physics and Center for Energy Science, Indian Institute of Science Education and Research, Pune-411008, India



(Received 9 February 2018; revised manuscript received 13 April 2020; accepted 14 April 2020; published 1 May 2020)

Using first-principles density functional theory (DFT +  $U$ ), we have investigated the possibility to tune the electronic and magnetic properties of the graphone/Ni(111) interface through O intercalation. Our study shows that the interaction of graphone becomes stronger with the Ni(111) surface as the coverage of intercalating O atoms is increased. Moreover, we find that as a function of O coverage, there is an interplay between the energy gained by O intercalation and the instability in the graphene sheet due to the presence of unsaturated C atoms which drives the reconstruction of the Ni surface at O coverages below 0.5 ML. With the increase in O coverage we find that there is huge enhancement in the magnetic moments on the Ni atoms at the interface. Most interestingly, for the interface at half a monolayer O coverage, we find that there is a significant enhancement in the magnetic moment of the graphone sheet that otherwise is quenched when adsorbed on the Ni(111) surface in absence of oxygen.

DOI: [10.1103/PhysRevB.101.195401](https://doi.org/10.1103/PhysRevB.101.195401)

### I. INTRODUCTION

Despite possessing several interesting properties like long mean free path of electrons, high electron mobility [1], etc., the use of graphene in electronic devices is greatly limited by the fact that it is a semimetal with zero band gap. Hence, there are efforts towards controllable band gap opening. One plausible way to achieve band gap opening is through chemical functionalization of the graphene sheet. For example, it has been shown that functionalizing graphene with a varying coverage of H atoms helps in achieving controllable band gap opening [2]. Moreover, it has also been predicted that when one side of the graphene sheet is completely hydrogenated (*graphone*) it becomes a ferromagnetic semiconductor with each unhydrogenated C atom having a magnetic moment of  $1.0 \mu_B$  [3]. The origin of the magnetic moment is attributed to the presence of localized unpaired  $p_z$  electrons that results from the breaking of the highly delocalized  $\pi$ -electron cloud of graphene due to the formation of -CH bonds [3].

In spite of the intriguing properties of graphone (GrH), its main drawback is that free standing GrH is unstable due to a huge sublattice imbalance, which arises due to the adsorption of hydrogen atoms on the carbon atoms of one sublattice of the graphene sheet [4,5]. Recently W. Zhao *et al.* have experimentally synthesized GrH on a Ni(111) substrate suggesting that graphone can be stabilized on transition metal surfaces [6]. Nevertheless, they did not study the magnetic properties of the supported graphone sheet. From our previous theoretical study of GrH supported on the Ni(111) surface

[Ni(111)/GrH], we find that GrH strongly interacts with Ni(111) that results in quenching of the interface magnetic moments. Not only are the magnetic moments on the C atoms quenched to  $0.04 \mu_B$ , but also those on the surface Ni atoms are reduced to  $0.16 \mu_B$  from  $0.71 \mu_B$  for the clean surface [7]. Retaining magnetic moment of Ni(111) surface is essential in order to design spintronic nanodevices, using the Ni(111)/GrH interface.

Oxygen intercalation between an adsorbate and substrate is shown to be an useful way to tune the interactions (both in terms of electronic properties and magnetic couplings) between them. For example, Bernien *et al.* [8] have shown that intercalating O between Fe-porphyrin molecules and ferromagnetic substrates results in an antiferromagnetic coupling between them. Studies of oxygen intercalation between graphene and its transition metal (TM) substrate show that the graphene sheet moves away and decouples from the substrate [9–11]. In particular, there have been several experimental studies using scanning tunneling microscopy (STM), angle resolved photoemission spectroscopy (ARPES), x-ray photoemission spectroscopy (XPS), Electron energy loss spectroscopy (EELS), etc., on the effect of oxygen intercalation on graphene supported on Ni(111) surface where the graphene sheet is chemisorbed on the Ni substrate [12–15]. All these experiments show that it is possible to intercalate O between the Ni substrate and the graphene sheet. They also observe formation of NiO layers, either the polar (111) or nonpolar (001) surfaces, depending on the temperature at which the samples are prepared. Most importantly, they show that similar to other substrates like Ir(111), Cu(111) on which the graphene sheet is physisorbed, in this case also O intercalation decouples the graphene sheet from the surface. This is corroborated

\*niharika.joshi@students.iiserpune.ac.in

by the observation of the Dirac cone in the ARPES spectra. Moreover, it was also observed that the graphene sheet is doped. While Bignardi *et al.* [13] observed a small amount of  $n$ -doping, Dedkov *et al.* [14] observed  $p$  doping in the graphene sheet. DFT based first-principles calculations of the Ni-O-graphene interface by Zhang *et al.* [17] supported the observations of Dedkov *et al.* Further, recently Jugovac *et al.* observed similar behavior when O is intercalated at the strongly interacting graphene-Co interface [16]. In contrast to graphene, for GrH, due to the presence of an unsaturated C atom, the interaction between the intercalated O and GrH will be stronger. Hence it would be interesting to explore the plausibility of tuning the interface properties of GrH/Ni(111) through varying amount of O intercalation. This motivated us to study the effect of O intercalation between GrH and the Ni(111) surface.

The rest of the paper is organized as follows. In Sec. II, we have described the details of the computational methods used in our calculations. The results from our calculations are presented and discussed in Sec. III. In this section, we also provide a plausible way of experimentally synthesizing these interfaces. Finally, we conclude in Sec. IV.

## II. METHODOLOGY

### A. Computational details

We have performed *ab initio* density functional theory (DFT) calculations using the plane-wave based QUANTUM ESPRESSO software [18]. The electron-ion interactions have been described using ultrasoft pseudopotentials [19]. The energy cutoffs used for wavefunction and charge density are 35 and 360 Ry, respectively. The electron-electron exchange-correlation potential is described by Perdew, Burke, and Ernzerhof parametrization of the generalized gradient approximation [20]. The Brillouin zone integrations are performed on a  $12 \times 12 \times 1$  shifted Monkhorst Pack  $k$ -point grid per  $(1 \times 1)$  Ni(111) surface unit cell [21]. To accurately calculate the small magnetic moments on the supported graphene, we have used a denser  $k$ -point grid of  $36 \times 36 \times 1$  per  $(1 \times 1)$  Ni(111) surface unit cell. To speed up the convergence, we have used Marzari-Vanderbilt smearing of width 0.005 Ry [22].

The Ni(111) surface unit cell is modelled by an asymmetric slab of six layers, of which the bottom three layers are kept fixed at the bulk interplanar distance while the top three layers are relaxed. The periodic images in the direction perpendicular to the surface are separated by a vacuum of 12 Å to minimize the spurious interaction between them. Additionally we have included dipole correction to remove the spurious long-range dipole interaction between the periodic images of the slab along the direction perpendicular to the surface.

In order to test the pseudopotentials, we have computed the lattice parameter and magnetic moment of bulk Ni, the bond length, and magnetic moment of oxygen molecule in gas phase, and the lattice parameter and C-C bond length in freestanding graphene. We have obtained the lattice parameter of bulk Ni to be 3.52 Å with magnetic moment of  $0.64 \mu_B$  per Ni atom. From our calculations, we find that the oxygen molecule is in a triplet ground state with an O-O bond length of 1.22 Å. For freestanding graphene, we have obtained the

lattice parameter to be 2.46 Å with C-C bond length of 1.43 Å. All these results are in excellent agreement with the previous reports [3,23–25].

### B. Determination of $U$

Since conventional GGA functionals do not correctly account for the exchange and correlation interactions between the Ni- $d$  electrons, particularly when they are interacting with O- $2p$  states (e.g., NiO), we have performed GGA +  $U$  calculations to determine the structure and electronic properties of this interface. In order to determine the value of  $U$ , we have used the linear response approach proposed by M. Cococcioni and S. Gironcoli [26]. In this method the value of the on-site Coulomb ( $U$ ) correction is given by the difference of the inverse of the interacting ( $\chi$ ) and noninteracting ( $\chi_0$ ) response of the occupation of the Ni- $d$  states to a small perturbing potential. The response function is given by

$$\chi^I = \frac{dn^I}{d\alpha^I} \quad \text{and} \quad \chi_0^I = \frac{dn_0^I}{d\alpha^I}, \quad (1)$$

where  $n^I$  is the occupation of atom I and  $\alpha$  is the potential shift. The subscript “0” denotes the noninteracting case.  $U$  is then given by

$$U = (\chi_0^I)^{-1} - (\chi^I)^{-1}. \quad (2)$$

In our system, the Ni atoms are in two different types of environment. The ones at the surface of the slab are interacting with both the Ni and O atoms, while those below the surface Ni layer, are interacting with neighboring Ni atoms only. Hence, to understand for which atoms the effect of  $U$  will be important, we have computed  $U$  for three cases: (i) bulk Ni, (ii) bulk NiO, and (iii) the surface Ni atom in Ni(111)/1 ML-O system using the linear response method described above. To determine the  $U$  for bulk Ni and bulk NiO, we used  $(3 \times 3)$  supercells. For the Ni(111)/1 ML-O we used a  $(2 \times 2)$  supercell. Figure 1 shows the change in the Ni- $d$  occupation as a function of perturbing potential in the interacting and noninteracting cases for the bulk NiO, bulk Ni, and Ni(111)/1 ML-O surface. The values of  $U$  obtained for these systems are 4.67, 6.84, and 9.18 eV, respectively. Our obtained value of  $U$  for NiO is in excellent agreement with that reported by Coccocini *et al.* [26].

While the lattice parameters obtained for bulk Ni with and without  $U$  (3.48 Å versus 3.52 Å) are similar, the magnetic moments are significantly different. While with GGA the magnetic moment on each Ni atom is about  $0.64 \mu_B$ , upon incorporating  $U$  it reduces to about  $0.48 \mu_B$ . We find that for bulk Ni the results without  $U$  correction are in excellent agreement with experiments. For the systems studied in this work, the Ni atoms from the second layer of the slab onwards are in an environment that is similar to the bulk. Since from our test calculations we find that the GGA +  $U$  correction does not correctly describe the Ni-bulk environment, for our system, we have applied GGA +  $U$  only for the surface Ni atoms that are interacting with O.

For the Ni(111)/1 ML-O, since our obtained value of  $U = 9.18$  eV is quite large, we also did the calculations for this system with  $U = 4.67$  eV. Figure 2 shows the density of states (DOS) projected on Ni- $d$  states of the Ni atoms at

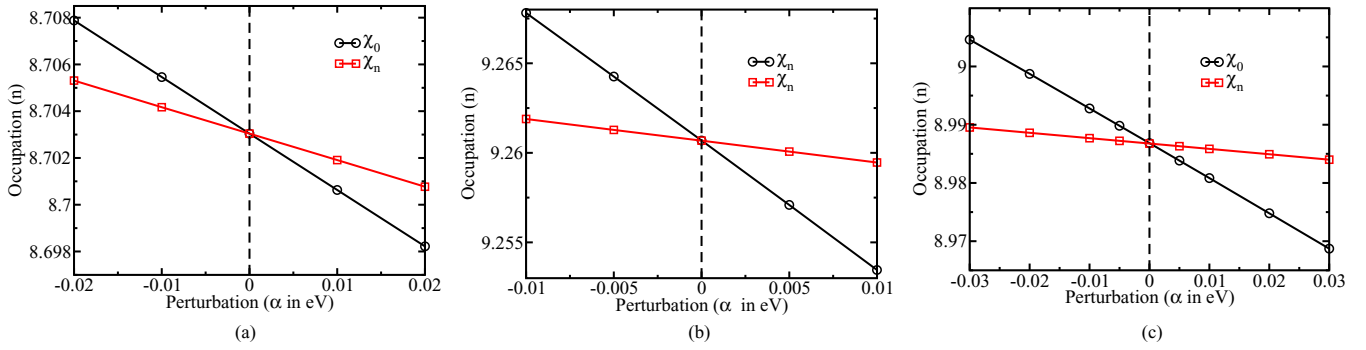


FIG. 1. Variation in the Ni- $d$  occupation in (a) NiO bulk, (b) Ni bulk, and (c) Ni(111)-O surface as a function of the perturbing potential ( $\alpha$ ).

the interface, O- $p$  and graphone electronic states computed with  $U = 0, 4.67$ , and  $9.18$  eV for Ni(111)/1 ML-O/GrH. We find that the localization effect due to the  $U$  correction results in a shift of the density of Ni- $d$  states towards lower energy compared to those obtained from GGA. In contrast, the shift in the DOS for O  $p$  states and that of graphone are much smaller. Additionally we also observe a depletion in the contribution to the DOS at the Fermi energy from not only the Ni  $d$  and O  $p$  states but also for the graphone. In particular, for the Ni  $d$  spin-down states, the decrease in DOS is quite significant. While the states around the Fermi energy are due to hybridization between Ni  $d$  and O  $p$ , the ones that are occupied (empty) have a predominantly O  $p$  (Ni  $d$ ) character. We note that both values of  $U$  give a qualitatively same picture. Hence, we have used  $U = 9.18$  eV for our calculations, which is the value of  $U$  obtained from the linear response calculations.

### C. Determination of energetics

To determine the stability of the O-intercalated Ni-GrH interface compared to that in the absence of oxygen we have computed the formation energy ( $E_f$ ), which is given by

$$E_f = \frac{E_{\text{Ni(111)-O/GrH}} - E_{\text{Ni(111)/GrH}} - \frac{N}{2} E_{\text{O}_2}}{A} \quad (3)$$

In the above equation,  $E_{\text{Ni(111)-O/GrH}}$  and  $E_{\text{Ni(111)/GrH}}$  are the total energies of the interface with and without O, respectively.  $E_{\text{O}_2}$  is the total energy of an oxygen molecule in the gas phase,  $N$  is the number of O atoms at the interface and  $A$  is the area

of the interface. A negative value of  $E_f$  implies that the O intercalated interface is more stable than the one without O.

Further, in order to understand how the interaction between the intercalated O atoms and C atoms of the graphone sheet affects the C-H bond strength in graphone, we have also computed the H binding energy ( $E_b$ ) that is given as

$$E_b = \frac{E_{\text{Ni(111)-O/GrH}} - E_{\text{Ni(111)-O/Gr}} - n E_{\text{H}}}{A} \quad (4)$$

In Eq. (4),  $E_{\text{Ni(111)-O/Gr}}$  and  $E_{\text{H}}$  are the total energies of the graphone sheet on Ni-O and a H atom in gas phase. Since graphone is prepared by adsorbing atomic H on graphene, we have considered the reference energy for H as that of an isolated H atom.  $n$  is the number of H atoms in the unit cell.

## III. RESULTS

### A. Validation of the method

Usually in most of the DFT +  $U$  based calculations for strongly correlated materials, the  $U$  correction is applied to all the atoms of a given species. However, in our case, atoms of the same species behave in two different ways. While for the Ni atoms that do not interact with O, the correlation effects described by PBE-GGA is sufficient, those on the surface and interacting with O require a more accurate description of the electron-electron exchange correlation effects. Hence we are using DFT +  $U$  only for the latter class of Ni atoms. Therefore, to verify and validate that our approach can correctly describe a physical system, we have studied the effect of O

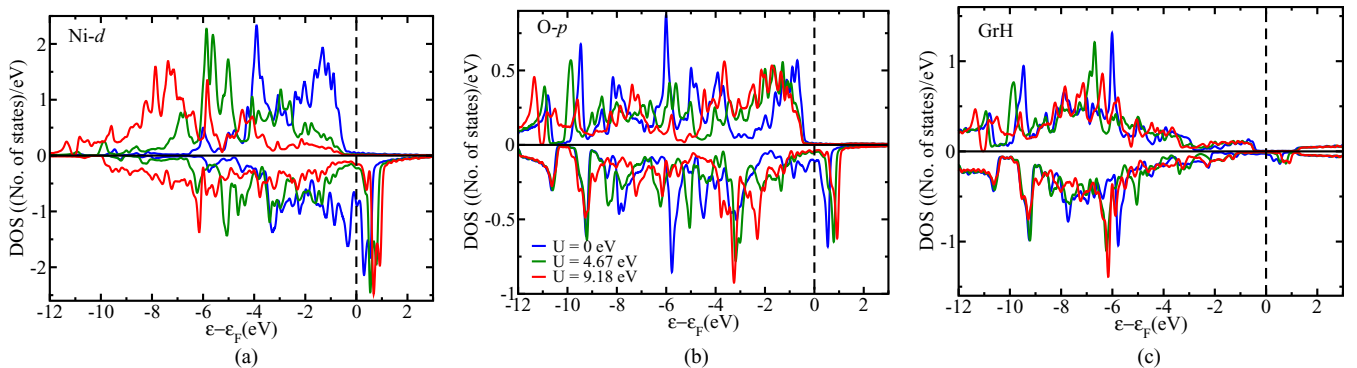


FIG. 2. Density of states projected on to (a) Ni  $d$  states of surface Ni atom, (b) O  $p$  states and (c) graphone in the Ni(111)-O/GrH interface with 1 ML O coverage. The blue, green, and red lines show plots for  $U = 0, 4.67$ , and  $9.18$  eV, respectively. The vertical dotted line shows the Fermi energy which is set at 0 eV.

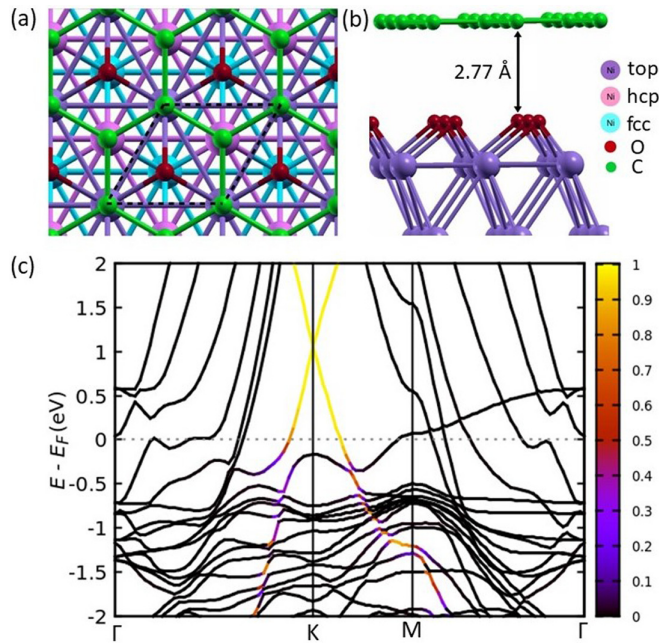


FIG. 3. (a) Top view and (b) side view of top-fcc configuration of Ni(111)/1 ML-O/GrH. Ni, C, O, and H atoms are denoted by purple, green, red, and magenta colors, respectively. In (a) for better visualization, the Ni atoms forming hcp and fcc sites are denoted by pink and cyan colors. Distance marked in the figures are in angstroms.

intercalation at the graphene/Ni(111) surface for which there are both experimental and theoretical results available.

The effect of O intercalation on the graphene/Ni(111) interface has been studied at 1.0 ML of O coverage. Previous studies have shown that the oxygen atoms preferably binds at the highly coordinated fcc-site on Ni(111) surface [27]. Hence for all the O coverages used in this paper, we have kept the O atoms on the Ni-fcc hollow site and determined the lowest energy adsorption configuration of graphene and GrH. Amongst the different possible adsorption configurations of graphene on the O covered surface, we find that the one in which the C atoms occupy the top and hcp sites [with respect to the Ni(111) surface] is lowest in energy [Figs. 3(a) and 3(b)]. The graphene sheet is about 2.77 Å away from the surface compared to that of 2.10 Å observed for the Ni-graphene interface [7]. These results, in accordance with the different experimental reports described in the Introduction, suggests that the graphene sheet is decoupled from the Ni substrate upon O intercalation.

Figure 3(c) shows the band structure of the O-intercalated interface projected on the  $C p_z$  states of graphene. In accordance with the ARPES results obtained by Dedkov *et al.*, we find that (a) the Dirac cone of the graphene sheet is almost recovered, further suggesting the weakening of the graphene-Ni interactions and (b) the Fermi level is about 1.00 eV lower in energy compared to the position of the Dirac cone, which is an indication of the graphene sheet being *p*-doped. We note that our estimate of the difference in position between the Fermi energy and graphene Dirac cone is about 0.3 eV larger compared to that observed by Dedkov *et al.* This can be

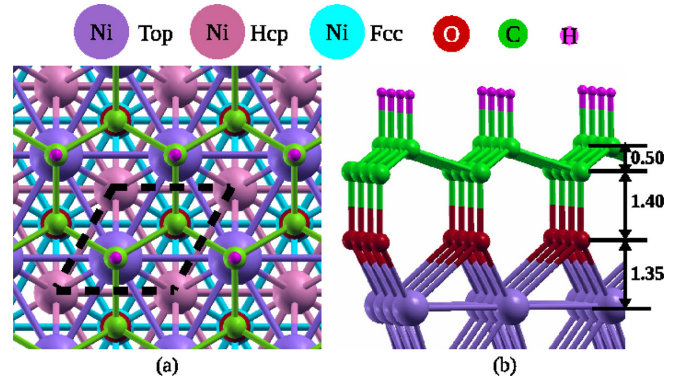


FIG. 4. (a) Top view and (b) side view of top-fcc configuration of Ni(111)/1 ML-O/GrH. Ni, C, O, and H atoms are denoted by purple, green, red and magenta colors, respectively. In (a) for better visualization, the Ni atoms forming hcp and fcc sites are denoted by pink and cyan colors. Distance marked in the figures are in angstroms.

attributed to the differences in the structure of the interface. While in our case we have a single layer of NiO(111) surface, which presumably is more reactive, in the experiments, there are a many layers of NiO present. These results suggests that indeed our proposed treatment of the exchange-correlation effect and our determined value of  $U$  can correctly describe the physics of the system.

## B. Structure and energetics

With the validation of our methodology in the previous section, we proceed to discuss the effect of O intercalation on the properties of GrH/Ni(111) O. We have studied intercalation of 0.25, 0.50, and 1.00 ML of O.

*1.0 ML O coverage.* In free standing GrH, there are two types of C atoms, namely, hydrogenated (C1) and unhydrogenated (C2). On the Ni(111)/1 ML-O surface, there are three available sites for the adsorption of carbon atoms in GrH, namely, top, hcp, and fcc sites. Therefore there are six possible configurations for the interface of Ni(111)/1 ML-O/GrH: (i) top-fcc, (ii) top-hcp, (iii) hcp-top, (iv) hcp-fcc, (v) fcc-top, and (vi) fcc-hcp. Throughout this paper we have followed the convention that in the name of the configurations the first (second) label represents the adsorption site of C1 (C2). For example, top-fcc means that the C1 atom is on a site that is directly above the Ni atom while the C2 C atom is occupying an fcc hollow site. In our previous study [7], we have shown that the fcc-top configuration of GrH (C1 at the fcc site and C2 at the top site) is most stable. Since C1 is already hydrogenated, it is unlikely that C1 will bind with the O at the fcc site. Therefore we have not considered fcc-top and fcc-hcp configurations. Amongst the remaining four configurations we find top-fcc and hcp-fcc configurations to be the most favourable ones with equal formation energies of  $-0.19 \text{ eV}/\text{\AA}^2$ . Figure 4 shows the top and side view of the relaxed top-fcc configuration. The H binding energies are  $-0.54 \text{ eV}/\text{\AA}^2$ . We note that this is more negative compared to that of  $-0.39 \text{ eV}/\text{\AA}^2$  in absence of O intercalation, thereby indicating that O intercalation strengthens the C-H bond. The

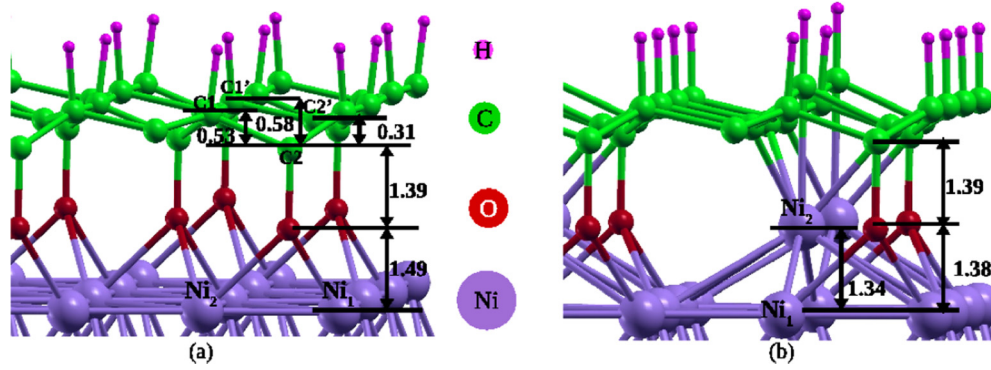


FIG. 5. Side-view top-fcc configuration of (b) Ni(111)/0.5 ML-O/GrH and (c) Ni(111)/0.25 ML-O/GrH. Ni, C, O, and H atoms are denoted by purple, green, red, and magenta colors, respectively. Distances marked in the figures are in angstroms.

strong binding of H to the Gr supported on O covered Ni surface is also reflected in the enhanced buckling of  $0.50 \text{ \AA}$  observed in GrH. The C-O bond length is about  $1.40 \text{ \AA}$  in both, top-fcc and hcp-fcc, configurations. We note that this is larger in comparison to the C-O bond length in CO molecule in gas phase ( $\sim 1.13 \text{ \AA}$ ) and that of CO molecule adsorbed on Ni(111) surface with C atom interacting with the surface ( $\sim 1.20 \text{ \AA}$ ) [28]. The Ni-O bond length is also increased to  $1.98$  and  $1.97 \text{ \AA}$  in top-fcc and hcp-fcc configurations, respectively, compared to that of  $1.85 \text{ \AA}$  observed in absence of GrH.

**0.50 ML O coverage.** To determine the structure of the interface in presence of  $0.5 \text{ ML O}$ , we have used a  $(2 \times 2)$  surface unit cell. This results in two O atoms in between the Ni(111) surface and GrH. Graphone can have four possible configurations: (i) two configurations with C1 at top site while C2 either at hcp (top-hcp) or fcc (top-fcc) site and (ii) two configurations with C1 at hcp site and C2 either at top (hcp-top) or fcc site (hcp-fcc). From our calculations we find that graphone prefers to adsorb on Ni(111) surface when oxygen atoms are present at fcc sites alone.

Similar to the interface with  $1 \text{ ML O}$  coverage, the Ni(111)/ $0.5 \text{ ML O/GrH}$  interface has two configurations, namely, top-fcc and hcp-fcc, that are lowest in energy, each having a formation energy of around  $-0.18 \text{ eV/\AA}^2$ .  $E_f$  is reduced compared to the  $1.0 \text{ ML O}$  case. At this O coverage the number of inequivalent C atoms in GrH increases to four, namely, those at the top site (or hcp site in hcp-fcc) with hydrogen adsorbed on them (C1 and C1'), the unhydrogenated ones at fcc-site (C2') that do not interact with O and the unhydrogenated ones at fcc site which directly interact with the oxygen atoms (C2), as shown in Fig. 5(a). The buckling between the planes of C1 and C2 is about  $0.53 \text{ \AA}$  and that of C2 and C1' is about  $0.58$  ( $0.57$ )  $\text{ \AA}$  in top-fcc (hcp-fcc) configuration. The buckling between C2 and C2' is about  $0.31 \text{ \AA}$  in top-fcc ( $0.30 \text{ \AA}$  in hcp-fcc configuration). Not only the GrH sheet is rumpled but also the Ni surface is slightly distorted due to the interaction with GrH. Out of the four surface Ni atoms in the  $(2 \times 2)$  unit cell, two bind to one oxygen atom ( $\text{Ni}_1$ ) and two binds to two oxygen atoms ( $\text{Ni}_2$ ). This results in a small rumpling of about  $0.01 \text{ \AA}$  ( $0.02 \text{ \AA}$ ) on the Ni surface in fcc-fcc:top-fcc (fcc-fcc:hcp-fcc) configuration. The binding energy of the H atoms reduces of to  $-0.39 \text{ eV/\AA}^2$  and is comparable with that observed in absence of the O atom.

**0.25 ML O coverage.** Upon further reducing the oxygen coverage to  $0.25 \text{ ML}$ , we again have four possible configurations (top-fcc, top-hcp, hcp-fcc, and hcp-top) of Ni(111)/O/GrH interface with O at the fcc site. We have excluded fcc-top and fcc-hcp configurations because placing C1 of GrH over O atoms is not feasible. Similar to the interface with  $1 \text{ ML}$  and  $0.50 \text{ ML}$  coverages we find top-fcc and hcp-fcc to be more stable configurations. However, in contrast with the other higher O coverages, at  $0.25 \text{ ML O}$  coverage we observe that  $1/4$  of the surface Ni atoms move outward by about  $1.34 \text{ \AA}$  in top-fcc configuration (Fig. 5). The shifted Ni atom ( $\text{Ni}_2$ ) directly interacts with the graphone sheet, as shown in figure 5(b) for top-fcc configuration. These pulled out Ni atoms and O atoms (in fcc site) form a rumpled NiO layer with rumpling of  $0.04 \text{ \AA}$  in top-fcc configuration. The graphone sheet is also highly puckered. Therefore we find that the formation energy of the interface and binding energy of H at  $0.25 \text{ ML}$  coverage of O are further reduced to  $-0.05$  and  $-0.22 \text{ eV/\AA}^2$ , respectively, in both, top-fcc and hcp-fcc configurations.

Table I summarizes the  $E_b$  and  $E_f$  values of the different configurations at each of the three O coverages. Interestingly, we find that the C-H bond strength is modulated by the O

TABLE I. Formation energy of the interface ( $E_f$ ) and binding energy of H ( $E_b$ ) on graphone supported on the Ni(111)-O surface at different O coverages and for different possible configurations.

O coverage	O position	C1 position	C2 position	$E_f$ ( $\text{eV/\AA}^2$ )	$E_b$ ( $\text{eV/\AA}^2$ )
1 ML	fcc	top	fcc	-0.19	-0.54
		top	hcp	0.16	-0.19
		hcp	fcc	-0.19	-0.54
		hcp	top	0.21	-0.14
0.5 ML	fcc-fcc	top	fcc	-0.18	-0.39
		top	hcp	0.17	-0.04
		hcp	top	0.03	-0.18
		hcp	fcc	-0.18	-0.39
0.25 ML	fcc	top	fcc	-0.05	-0.22
		top	hcp	0.17	0.01
		hcp	top	0.11	-0.06
		hcp	fcc	-0.05	-0.22

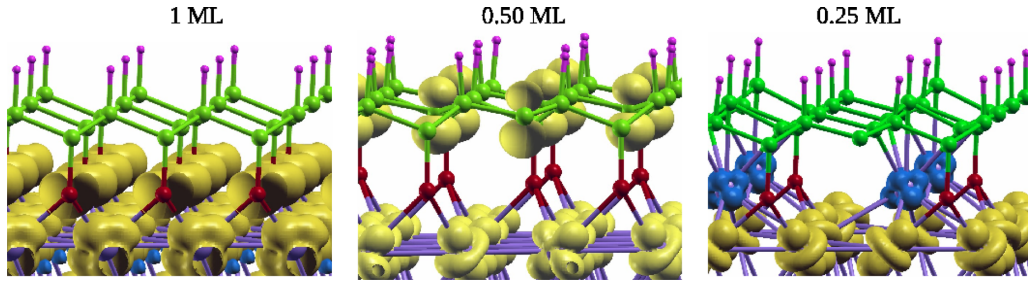


FIG. 6. Magnetization density ( $\Delta m = n^\uparrow - n^\downarrow$ ) at the interface of graphone and Ni(111) surface with (a) 1, (b) 0.50, and (c) 0.25 ML O coverages. The yellow and blue isosurfaces represents positive (spin-up) and negative (spin-down) net magnetization ( $\Delta m$ ). The isovalue is around  $0.02 e^-/\text{\AA}^3$ .

coverage at interface. At 1.0 ML O coverage, the C-H bonds are stronger compared to that in absence of O. Upon reducing the O coverage to 0.5 ML, the bond strength is reduced and is same as that in absence of O atom. Further reduction of the O-coverage results in weakening of the bond compared to that observed in absence of O. Moreover, in all three O coverages, we find that top-fcc and hcp-fcc configurations are equally favourable and the geometry of these two configurations are also similar. The difference in these two configurations is only in the position of the hydrogenated C atom of graphone which does not actively participate in the interaction with the substrate atoms. Hence, we find that both the configurations show similar properties. Therefore further we have discussed the results obtained for only top-fcc configuration of the Ni(111)/O/GrH interface at different O coverages.

To ascertain whether the surface reconstruction at low O coverages is induced by interactions with the graphone sheet, we took the reconstructed O covered Ni surface in the same geometry as with GrH and relaxed the structure. We find that upon relaxation the surface goes back to the unreconstructed form thereby confirming that the strong interaction between GrH and the surface induces reconstruction of the oxygenated Ni(111) surface. The driving force for this reconstruction can be attributed to the minimization of GrH sublattice imbalance to enhance its stability. On clean Ni(111) surface all the unhydrogenated C atoms of GrH form bonds with Ni atoms. This configuration results in removal of sublattice imbalance making GrH stable. Similarly for the 1.0 ML coverage, each of the unhydrogenated C atoms forms C-O bonds with the interface O. Hence in this case also there is no sublattice imbalance and no reconstruction is observed. However, at 0.25 ML O coverage, at the unreconstructed interface, 3/4 of the unhydrogenated C atoms cannot form bonds either with Ni or O; GrH remains unstable. To minimize this imbalance and thereby enhance its stability, GrH induces reconstruction of the Ni(111) surface such that maximum possible number of unhydrogenated C atoms can form bonds. In this context, it is intriguing that the Ni surface is not reconstructed at 0.5 ML O coverage where there is still unsaturated C atoms in the graphone sheet. To understand this, it is instructive to compare the  $E_b$  between 0 and 0.5 ML O coverage. In absence of any intercalated O (0 ML O coverage), the lattice imbalance in the graphone sheet is zero because each C atom is either bound to a Ni or a H atom. Hence, the  $E_b$  for this case, which is  $-0.39 \text{ eV}/\text{\AA}^2$ , provides a lower bound of the energy that needs to be gained by the system on O intercalation that

will stabilize the graphone lattice. For cases where the energy gain is less than above, the lattice instability will drive the reconstruction. For the particular case of 0.5 ML O coverage, we find that  $E_b$  is exactly same as that in absence of O. The moment the O coverage is reduced, the instability takes over and induces reconstruction of the Ni(111) surface as observed in case of 0.25 ML coverage.

### C. Magnetic properties at the Ni(111)/O/graphone interface

Figure 6 shows the magnetization density plots for the Ni(111)/O/GrH interface with 1, 0.50, and 0.25 ML O coverages, respectively. In Ni(111)/O 1ML/GrH, we have obtained a small magnetic moment of about  $0.02 \mu_B/\text{C}$  atoms on GrH, which is contributed by the C1 atoms. The magnetic moment on GrH is aligned parallel with respect to the magnetic moment of the surface Ni atoms. This is in contrast to what we had observed in the absence of the intercalating O atoms where we had found a small magnetic moment of about  $-0.02 \mu_B/\text{C}$  atom orientated antiparallel with respect to the magnetic moments on the surface Ni atoms [7]. The intercalation of oxygen atoms not only modifies the magnetic coupling between the carbon atoms of graphone and surface Ni atoms but also results in more than *sevenfold* enhancement of the magnetic moments on surface Ni atoms. While the magnetic moment on the Ni atoms are quenched upon adsorption of GrH to  $0.16 \mu_B/\text{Ni}$  atom [7] from that of  $0.71 \mu_B/\text{Ni}$  atom for the clean surface, we find that on O intercalation, the magnetic moment of the surface Ni atoms increases to about  $1.13 \mu_B/\text{Ni}$  atom [about 45% enhanced with respect to that in the clean Ni(111) surface]. The Ni atoms in the second and third layers below the top one show small reduction of magnetic moment of around 7% and 3%, respectively, with respect to their moments in clean surface. The magnetic moments in the remaining Ni(111) layers are unchanged compared to that in the clean Ni(111) surface.

Upon reducing the O coverage to 0.50 ML and then further to 0.25 ML we notice that the magnetic moments on the surface Ni atoms also decreases. In Ni(111)/O 0.50 ML/GrH interface, the magnetic moments on Ni<sub>1</sub> and Ni<sub>2</sub> are nearly same,  $0.98 \mu_B$ . The average magnetic moment ( $0.98 \mu_B/\text{Ni}$  atom) is slightly smaller than that obtained with 1 ML oxygen coverage but still about six times greater than what is observed in the absence of the intercalating oxygen layer [7]. The magnetic moments on hydrogenated C (C1 and C1') and C2 carbon atoms are about  $-0.06 \mu_B$  and  $0.04 \mu_B$ , respectively,

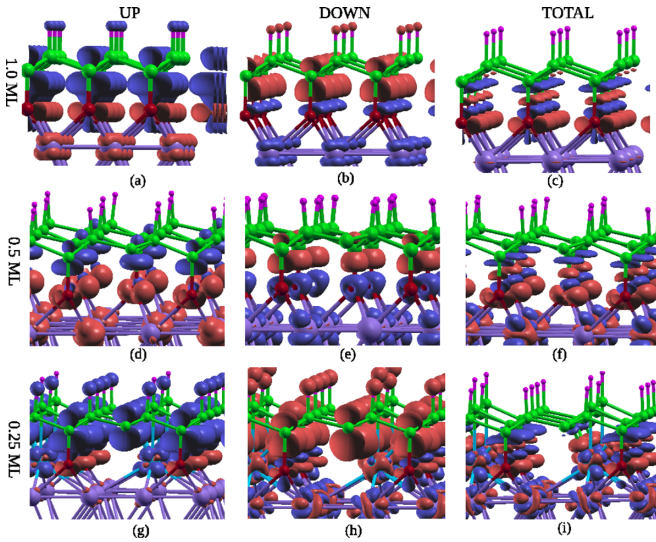


FIG. 7. Spin-resolved and total charge transfer at the interface of graphone and Ni(111) surface with 1.0, 0.5, and 0.25 ML O coverage. The red and blue isosurface represents charge accumulation and depletion, respectively. The isovalue is around  $0.02 e^-/\text{\AA}^3$ .

while that on  $C2'$ , with a dangling bond, is around  $0.72 \mu_B$ . This results in an average moment of about  $0.17 \mu_B$  per C atom in GrH, which is *eight* times greater than the average moment of GrH on clean Ni(111) surface. In Ni(111)/O 0.25 ML/GrH, the magnetic moments of the undisplaced Ni ( $Ni_1$ ) and displaced Ni ( $Ni_2$ ) atoms have antiparallel orientations and their magnitudes are about  $0.96$  and  $-0.36 \mu_B$ , respectively. The magnetic moment on carbon atoms which are hydrogenated or are bound to oxygen atom are negligible. The remaining carbon atoms that interacts with  $Ni_2$  atoms have a small magnetic moment of about  $-0.06 \mu_B$  aligned ferromagnetically with respect to that of  $Ni_2$ .

#### D. Charge transfer at the Ni(111)/O/graphone interface

To understand the enhancement of the magnetic moments of the surface Ni atoms due to O intercalation, we have plotted spin-resolved and total charge transfer at different O coverages. The isosurfaces for the same are shown in Fig. 7. We find that the direction of charge transfer is dependent on the spin polarization. While for the spin up channel, we find that electrons are transferred from GrH to Ni, for the spin down channel we find the charge transfer occur in the reverse direction. This results in a net accumulation of spin-up electrons on the surface Ni atoms resulting in seven fold increase in the magnetic moment at 1 ML O coverage. However, this net accumulation of spin-up electrons decreases on Ni(111) surface with decrease in O coverage, thereby resulting in a decrease in the magnetic moment on the Ni atoms at lower O coverages. For the 0.25 ML O coverage, the interface with reconstructed Ni(111) surface shows two types of charge transfer. While a charge transfer similar to that described above is seen for the undisplaced  $Ni_1$  atoms, the displaced  $Ni_2$  atoms show charge transfer in reverse direction.  $Ni_2$  atoms accept spin-down electrons and donates spin-up electrons which is similar to the charge transfer observed at

TABLE II. Work function ( $\phi$ ) and surface dipole density ( $p$ ) of the Ni(111)-O surface before (with subscript “0”) and after adsorption of graphone. The positive and negative values of surface dipole densities indicates outwards and inwards orientation, respectively.

O coverage (ML)	$\phi$ (eV)	$\phi_0$ (eV)	$p$ ( $D/\text{\AA}^2$ )	$p_0$ ( $D/\text{\AA}^2$ )
0	4.01	5.03	0.03	0.00
0.25	3.64	6.37	0.07	-0.05
0.50	3.24	7.52	0.11	-0.08
1.00	1.93	8.07	0.16	-0.09

the interface of Ni(111) surface and GrH in the absence of oxygen atoms [7]. We note that this particular Ni atom is interacting directly with the C atoms of GrH. Thus our results indicate that varying the O coverage provides a handle to tune the charge transfer at the interface, which thereby gives rise to interesting magnetic and electronic properties of the interface.

Table II shows the changes in the work function of the Ni(111) surface for different O coverages, both with ( $\phi$ ) and without ( $\phi_0$ ) graphone. We find that in absence of GrH,  $\phi_0$  increases as the O coverage increases. However, in presence of graphone, we not only find a decrease in the work function (4.0 eV versus 5.03 eV, with and without GrH at 0 ML O) but also the trends as a function of O coverage is reversed. In contrast to that observed without GrH, we find that upon adsorbing GrH,  $\phi$  decreases as the O-coverage increases. The changes in the work function of a material ( $\Delta\phi$ ) is typically related to the changes in the surface dipole density  $\Delta p$  and is [29,30] given by

$$\Delta\phi = -\frac{e}{\epsilon_0} \Delta p, \quad (5)$$

where  $e$  and  $\epsilon_0$  are the charge of an electron and vacuum permittivity, respectively. For our system, these changes in the trends and magnitudes of work function implies that not only the magnitude but also the direction of the surface dipole density is changed upon adsorbing GrH. Interaction of an adsorbate with the substrate changes the dipole moment through charge transfer/redistribution ( $p_{\text{redist}}$ ) between substrate and adsorbate and through charge redistribution due to changes in the geometry of the substrate ( $p_{\text{sub}}$ ) and the adsorbate ( $p_{\text{ads}}$ ). Hence, we can write  $\Delta p$  as

$$\Delta p = p_{\text{redist}} + p_{\text{sub}} + p_{\text{ads}}. \quad (6)$$

$p_{\text{redist}}$  in the above equation is given by

$$p_{\text{redist}} = \frac{-e}{A} \int_0^c \Delta n(z) z dz, \quad (7)$$

where

$$\Delta n(z) = n_{NiOGrH}(z) - n_{NiO}(z) - n_{GrH}(z). \quad (8)$$

$A$  and  $c$  in Eq. (7) are the area and height of the unit cell, respectively.  $\Delta n(z)$  is the planar average [ $n(z) = \frac{1}{A} \int_0^a dx \int_0^b n(x, y, z) dy$ ] of the charge transfer which is defined in Eq. (8). The three terms in Eq. (8) are the planar averages of the charge density of the oxygenated Ni(111) surface with epitaxial graphone ( $n_{NiOGrH}$ ), the oxygenated Ni(111) surface in the same geometry as in the presence

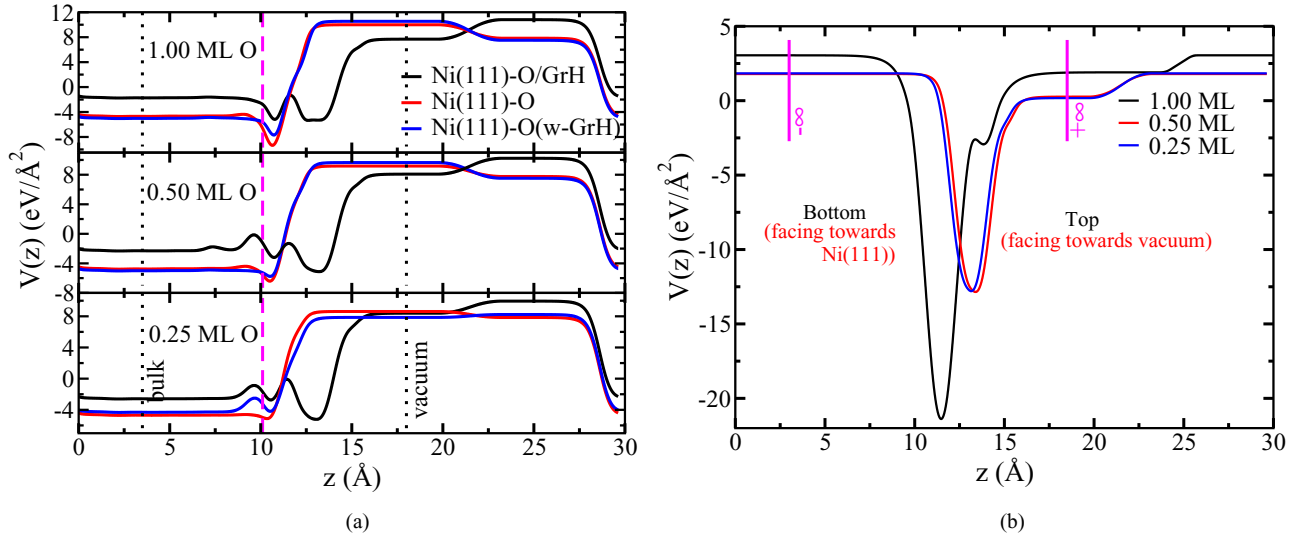


FIG. 8. (a) Macroscopic average of the electrostatic potential of Ni(111)-O surface when (i) with the adsorbed graphone (black), (ii) fully relaxed (red), and (iii) in the geometry as with graphone (blue) with different oxygen coverages. The two dotted vertical black lines show  $z$  value of bulk and vacuum chosen to determine  $V(\text{bulk})$  and  $V(\text{vacuum})$ . In the same plot, the magenta dashed line shows the approximate position of top Ni(111) layer and the zero of  $x$  axis denotes the bottom most Ni(111) layer. (b) Macroscopic average of the electrostatic potential of freestanding graphone in the geometry as on the Ni(111)-O surface with different O coverages. The magenta vertical lines in (b) show the  $z$  values chosen to determine  $V(\pm\infty)$ .

of graphone ( $n_{\text{NiO}}$ ) and graphone in the same geometry as when deposited on the oxygenated Ni(111) surface ( $n_{\text{GrH}}$ ), respectively.

The dipole density due to the structural changes occurring at the surface on adsorption of another material ( $p_{\text{sub}}$ ) is given by the difference between the dipole densities of the oxygenated Ni(111) surface when it is in the same geometry as in the presence of graphone ( $p'_{\text{Ni(111)-O}}$ ) and when it is fully relaxed ( $p_{\text{Ni(111)-O}}$ ) and is expressed as

$$p_{\text{sub}} = p'_{\text{Ni(111)-O}} - p_{\text{Ni(111)-O}}. \quad (9)$$

The dipole density in each case is determined as,  $p = \epsilon_0[V_{\text{vacuum}} - V_{\text{bulk}}]$ , where,  $V$  is the electrostatic potential at vacuum and bulk, respectively, as shown in Fig. 8(a).

The last term in Eq. (6), i.e., the dipole density of the adsorbate ( $p_{\text{abs}}$ ) in the same geometry as when it is deposited on the surface and can be written as

$$p_{\text{abs}} = \epsilon_0(V(+\infty) - V(-\infty)). \quad (10)$$

$V(\pm\infty)$  is defined in Fig. 8(b).

Figure 9 shows the variation in  $\Delta p$  for Ni(111)-O/GrH and its three components with increase in O coverage. In absence of GrH, the surface dipole of the O covered Ni surface points inwards. However, due to the interaction with the graphone sheet, the surface dipole moments reverse their direction and point away from the surface. As a function of O coverage, the magnitude of the surface dipole density increases from 0.02 to 0.16  $\text{D}/\text{\AA}^2$ . Among the three constituent terms we find that the largest contribution to the surface dipole density is from  $p_{\text{redist}}$ . Additionally, consistent with the direction of charge transfer observed, we find that the magnitude of  $p_{\text{redist}}$  is positive.  $p_{\text{abs}}$  shows smaller variation with its value lying in the range of  $-0.04$  and  $-0.05 \text{ D}/\text{\AA}^2$  as the O coverage is increased.

### E. Electronic properties at the Ni(111)/O/graphone interface

Figures 10(a), 10(d) and 10(g) show the plots of the DOS projected on GrH, Ni  $d$  of the Ni atoms at the interface and O  $p$  atoms with 1.00, 0.50, and 0.25 ML of O coverage, respectively. At 1.0 ML coverage, the interaction between GrH and Ni atoms are mediated through the interfacial O atoms. At the Fermi energy, for the spin up channel, we observe that all the surface Ni  $d$  states are below Fermi energy while there is a very small contribution of Ni  $d$  states in the spin down channel. The  $U$  shifts the Ni  $d$  states towards lower energy that results in reduction of hybridization with the O states. Between  $-12$  to  $-6 \text{ eV}$ , the contribution to the DOS comes primarily from the Ni  $d$  states. Above  $-6 \text{ eV}$ , there is mixing of the Ni  $d$  with O  $p$ . Above the Fermi energy, we observe

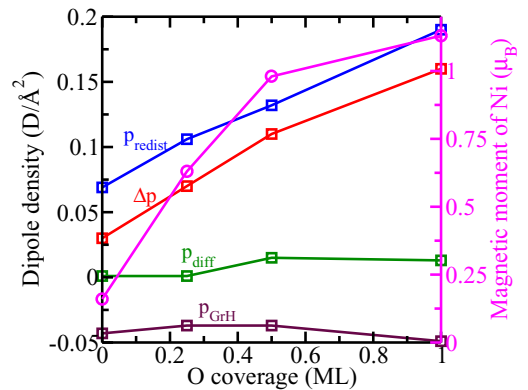


FIG. 9. Plot of the variation of surface dipole density (and its components) and net magnetic moment on the surface Ni atom as a function of O coverage. The y axis on the left-hand side of the figure is for the dipole density while that on the right is for magnetic moment.



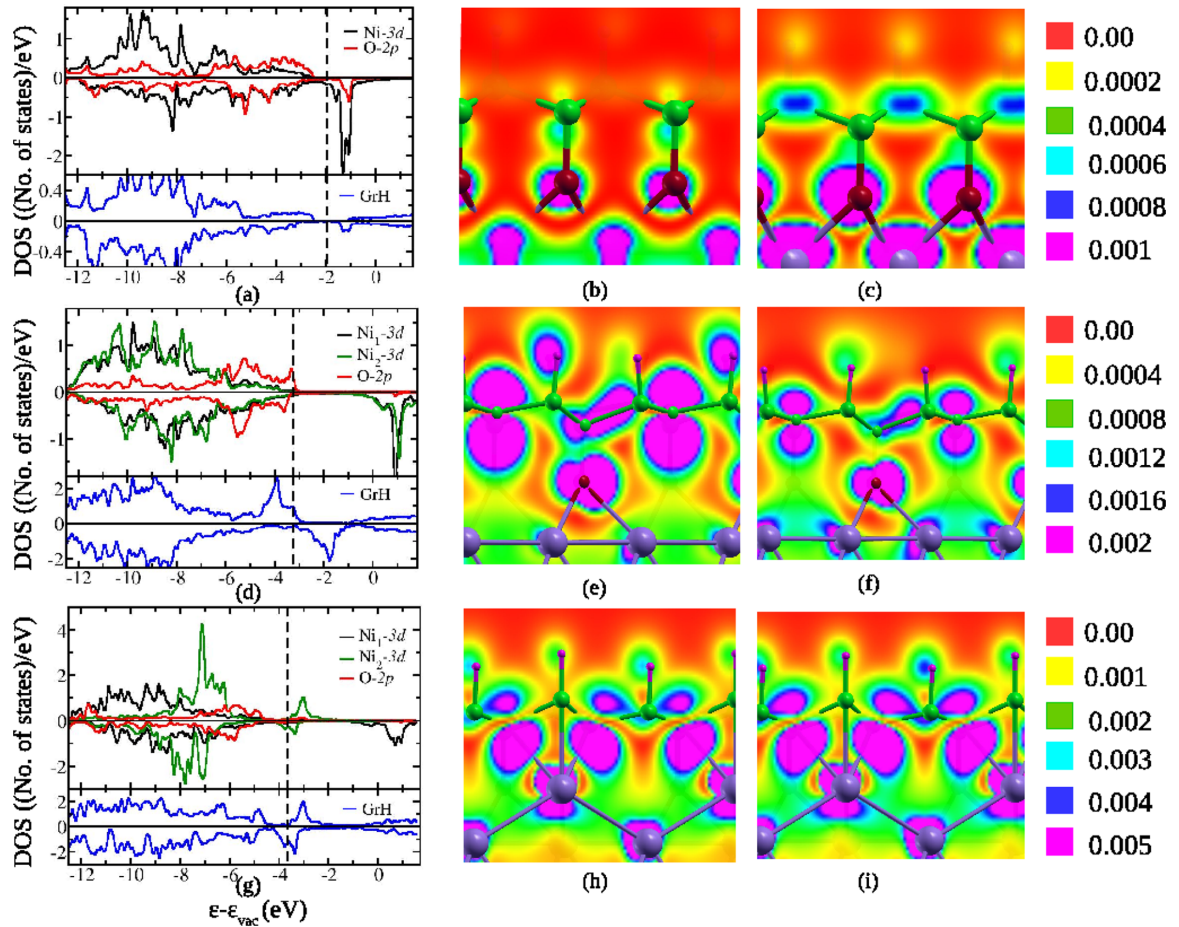


FIG. 10. Spin-resolved density of states [(a), (d), and (g)] and integrated local density of states in the energy range of  $E_f - 0.5$  to  $E_f + 0.5$  eV in spin-up channel [(b), (e), and (h)] and spin-down channel [(c), (f), and (i)] for the Ni(111)/O/GrH interface at 1 ML (top row), 0.5 ML (middle row), and 0.25 ML (bottom row) O coverage. In DOS plots, the states of Ni  $3d$  (black and green), O  $2p$  (red), and sum of C  $2s$ , C  $2p$ , and H  $1s$  (blue) are plotted. The vertical dotted line denotes the Fermi level. The energies are shifted with respect to vacuum energy.

empty Ni  $d$  states in the spin down channel only. These are primarily the  $d_{yz}$  and  $d_{zx}$  orbitals with a small contribution also from the  $d_{xy}$  and  $d_{x^2-y^2}$ . These results are consistent with the large magnetic moment observed in our calculations. We do not find any GrH states at the Fermi energy. As the O coverage is reduced to 0.5 ML, the basic feature of the DOS remains similar. However, in contrast with that at 1.0 ML coverage, we do not observe any Ni  $d$  or O  $p$  states at the Fermi energy. Again for the spin-up channel, all the Ni  $d$  states are occupied while for the spin down channel, there are empty Ni states, in accordance with the large magnetic moment observed for this case. However here, the two Ni atoms behave differently. While for Ni<sub>1</sub> the empty spin down states are primarily from  $d_{yz}$ , for Ni<sub>2</sub> these are predominantly from  $d_{zx}$ . Additionally we find GrH states at the Fermi energy. For the reconstructed surface at 0.25 ML coverage, the interaction between the Ni<sub>1</sub> atoms (those which are not pulled out of the surface) and the O atoms for the 0.25 ML coverage are similar to that observed for 1.0 and 0.5 ML coverage. In this case, empty states in the spin down channel are primarily from the  $d_{yz}$  orbitals. The Ni<sub>2</sub> (those that are pulled out of the surface)  $d$  states are more localized compared to those of Ni<sub>1</sub> and are more

or less completely filled in both the spin channel resulting in a reduced magnetic moment observed on these atoms. We also observe some states at the Fermi energy from GrH.

Since the electronic states of the spin up and spin down channel of this interface show different behavior, there might be a possibility of spin polarized conduction at these interfaces. To explore this, we have computed the integrated local density of states (ILDOS) in the energy range of  $E_f - 0.5$  eV to  $E_f + 0.5$  eV for all the three O coverage. The ILDOS plots are shown in Fig. 10. In order to have a continuous transport channel the electronic states need to span the whole region between the electrode. For the 1.0 ML coverage, we find that the spin up states [Fig. 10(b)] are primarily localized along the C-O, O-Ni bonds. In contrast, the spin down states are more delocalized throughout the space [Fig. 10(c)]. This suggests that at this interface there is a possibility of a spin-polarized current. However, for 0.5 ML [Figs. 10(e) and 10(f)] and 0.25 ML [Figs. 10(h) and 10(i)], the electronic states for both the spin up and spin down channel are delocalized throughout the interface. Hence for these interfaces the probability of having spin polarized transport is less compared to that for 1.0 ML O coverage.

### F. Experimental outlook for the synthesis of the Ni(111)/O/GrH interface

For realising the viability of the results obtained through computational techniques, it is important to relate the computational modeling of a desired system with the latest experimental techniques of material synthesis. In this paper, we propose a plausible way to fabricate the proposed Ni(111)-O/GrH interface. The structure and energetics at the interface are hence majorly influenced from the following experimental method for fabricating O-intercalated interface of Ni(111) and GrH. It has been shown earlier that single layer graphene can be successfully grown on the Ni thin-film substrate [31]. Also, the oxygen-covered Ni substrate can be achieved by so called surfactant-mediated growth method [8,32–34]. Thus, based on earlier reports, a step-by-step experimental prototype can be proposed as (i) deposition of, for example, 10 ML of Ni on a W(110) single crystal, (ii) dosing of O<sub>2</sub> gas (say 15 Langmuir), (iii) deposition of another 10 ML of Ni, (iv) growth of graphene layer, (v) hydrogenation of the graphene layer i.e. formation of graphone, and (vi) finally, heating-up of the system at elevated temperature, for example, 250 °C to make the Ni(111)-O/GrH interface. Notably, the dosing of O<sub>2</sub> gas can be controlled, which will allow us to tune the interfacial coverage of oxygen vis-à-vis magnetic coupling across the interface.

### IV. CONCLUSION

In summary, using GGA + *U* calculations, we have shown that the properties of Ni(111) surface and GrH interface can be tuned by intercalating O atoms between them. Our results show that there is a subtle balance between the energy gain

due to O intercalation and the instability in the graphene sheet due to sublattice imbalance. From our calculations, we show that below 0.5 ML coverage and in particular at 0.25 ML coverage the graphene lattice instability induces reconstruction of the Ni surface. In addition to the structural changes, we also observe significant changes in the magnetic properties of the interface. At 1 and 0.5 ML O coverage, the magnetic moments of the surface Ni atoms at the interface are significantly enhanced compared to the clean Ni(111) surface. Interestingly, for the 0.5 ML O coverage, we find the magnetic moment of the graphone sheet is also larger by an order of magnitude compared to that observed in absence of O. Our results indicates that the 1 ML and 0.5 ML O coverage interface may be promising candidates from spintronics applications. We hope that our work will motivate experimentalists to prepare these systems.

### ACKNOWLEDGMENTS

The authors would like to acknowledge CDAC, Pune, India and Center for Modeling and Simulation, University of Pune, India and CCMS, IMR, Tohoku University, Japan for providing computational facility. N.J. would like to acknowledge Indian Institute of Science Education and Research (IISER) Pune for scholarship. P.G. would like to acknowledge Department of Science and Technology (DST)-Nanomission, India Grants No. SR/NM/NS-1285/2014 and No. SR/NM/NS-15/2011 for funding. P.G. would also like to thank the International Center for Theoretical Physics (ICTP) Research Associate Program that provided him an opportunity to visit the center. The manuscript was written and finalized during one such visit.

- 
- [1] A. Geim and K. Novoselov, *Nat. Mater.* **6**, 183 (2007).  
 [2] J. O. Sofo, A. S. Chaudhari, and G. D. Barber, *Phys. Rev. B*, **75**, 153401 (2007).  
 [3] J. Zhou, Q. Wang, Q. Sun, X. Chen, Y. Kawazoe, and P. Jena, *Nano Lett.* **9**, 3867 (2009).  
 [4] L. Feng and W. X. Zhang, *AIP Adv.* **2**, 042138 (2012).  
 [5] Ž. Šljivančanin, R. Balog, L. Hornekær, *Chem. Phys. Lett.* **541**, 70 (2012).  
 [6] W. Zhao, J. Gebhardt, F. Späth, K. Gotterbam, C. Gleichweit, H. Steinrück, A. Görling, and C. Papp, *Chem. Eur. J.* **21**, 3347 (2015).  
 [7] N. Joshi, N. Ballav, and P. Ghosh, *Phys. Rev. B* **86**, 121411(R) (2012).  
 [8] M. Bernien, J. Miguel, C. Weis, M. E. Ali, J. Kurde, B. Krumme, P. M. Panchmatia, B. Sanyal, M. Piantek, P. Srivastava, K. Baberschke, P. M. Oppeneer, O. Eriksson, W. Kuch, and H. Wende, *Phys. Rev. Lett.* **102**, 047202 (2009).  
 [9] L. Ma, X. Zeng, and J. Wang, *J. Phys. Chem. Lett.* **6**, 4099 (2015).  
 [10] S. Gottardi, K. Müller, L. Bignardi, J. Moreno-Lopez, T. Pham, O. Ivashenko, M. Yablonskikh, A. Barinov, J. Björk, P. Rudolf, and M. Stöhr, *Nano Lett.* **15**, 917 (2015).  
 [11] E. Grånäs, J. Knudsen, U. A. Schröder, T. Gerber, C. Busse, M. A. Arman, K. Schulte, J. N. Andersen, and T. Michely, *ACS Nano* **6**, 9951 (2012).  
 [12] N. Ligato, L. S. Caputi, and A. cupolillo, *Carbon* **100**, 258 (2016).  
 [13] L. Bignardi, P. Lacovig, M. M. Dalmiglio, F. Orlandi, A. Ghafari, L. Petaccia, A. Baraldi, R. Larciprete, and S. Lizzit, *2D Mater.* **4**, 025106 (2017).  
 [14] Y. Dedkov, W. Klesse, A. Becker, F. Spath, C. Papp, and E. Voloshina, *Carbon* **121**, 10 (2017).  
 [15] S. L. Kovalenko, B. V. Andryushechkin, and K. N. Eltsov, *Carbon* **164**, 198 (2020).  
 [16] M. Jugovac, F. Genuzio, T. O. Montes, A. Locatelli, G. Zamborlini, V. Feyer, and C. M. Schneider, *Carbon* **163**, 341 (2020).  
 [17] W.-B. Zhang and C. Chen, *J. Phys. D* **48**, 015308 (2015).  
 [18] P. Giannozzi, S. Baroni, N. Bonini, M. Calandra, R. Car, C. Cavazzoni, D. Ceresoli, G. Chiarotti, M. Cococcioni, I. Dabo, A. Dal Corso, S. de Gironcoli, S. Fabris, G. Fratesi, R. Gebauer, U. Gerstmann, C. Gougoussis, A. Kokalj, M. Lazzeri, L. Martin-Samos, N. Marzari, F. Mauri, R. Mazzarello, S. Paolini, A. Pasquarello, L. Paulatto, C. Sbraccia, S. Scandolo, G. Sclauzero, A. Seitsonen, A. Smogunov, P. Umari, and R. Wentzcovitch, *J. Phys.: Condens. Matter* **21**, 395502 (2009).  
 [19] D. Vanderbilt, *Phys. Rev. B* **41**, 7892 (1990).  
 [20] J. P. Perdew, K. Burke, and M. Ernzerhof, *Phys. Rev. Lett.* **77**, 3865 (1996).  
 [21] H. Monkhorst and J. Pack, *Phys. Rev. B* **13**, 5188 (1976).

- [22] N. Marzari, D. Vanderbilt, A. De Vita, and M. C. Payne, *Phys. Rev. Lett.* **82**, 3296 (1999).
- [23] N. Ashcroft and N. Mermin, *Introduction to Solid State Physics*, 5th ed. (Harcourt College Publishers, New York, 1976).
- [24] P. Balbuena and V. Subrahmanian, *Theory and Experiments in Electrocatalysis* (Springer, New York, 2010).
- [25] S. López-Moreno and A. Romero, *J. Chem. Phys.* **142**, 154702 (2015).
- [26] M. Cococcioni and S. de Gironcoli, *Phys. Rev. B* **71**, 035105 (2005).
- [27] T. Li, B. Bhatia, and D. Sholl, *J. Chem. Phys.* **121**, 10241 (2004).
- [28] M. Gajdoš, A. Eichler, and J. Hafner, *J. Phys.: Condens. Matter* **16**, 1141 (2004).
- [29] T. C. Leung, C. L. Kao, W. S. Su, Y. J. Feng, and C. T. Chan, *Phys. Rev B* **68**, 195408 (2003).
- [30] A. Michaelides, P. Hu, M.-H. Lee, A. Alavi, and D. A. King, *Phys. Rev. Lett.* **90**, 246103 (2003).
- [31] C. F. Hermans, K. Tarafder, M. Bernien, A. Krüger, Y. Chang, P. M. Oppeneer, and W. Kuch, *Adv. Mater.* **25**, 3473 (2013).
- [32] C. Sorg, N. Ponpandian, M. Bernien, K. Baberschke, H. Wende, and R. Q Wu, *Phys. Rev. B* **73**, 064409 (2006).
- [33] D. Chylarecka, C. Wäckerlin, T. K. Kim, K. Müller, F. Nolting, A. Kleibert, N. Ballav, and T. A. Jung, *J. Phys. Chem. Lett.* **1**, 1408 (2010).
- [34] C. Wäckerlin, J. Nowakowski, S. Liu, M. Jaggi, D. Siewert, J. Girovsky, A. Shchyrba, T. Hählen, A. Kleibert, P. M. Oppeneer, F. Nolting, S. Decurtins, T. A. Jung, and N. Ballav, *Adv. Mater.* **25**, 2404 (2013).